University of Baghdad
College of Engineering
JOURNAL OF ENGINEERING

Journal of Engineering
journal homepage: www.joe.uobaghdad.edu.iq
Number 12 Volume 26 December 2020

Mechanical and Energy Engineering

Simulation and Experimental Walking Pattern Generation for Two Types of Degrees of Freedom Bipedal Locomotion Robot

Ali Fawzi Abdul Kareem *
Ph.D. student
University of Baghdad/College of Engineering\
Mechanical Engineering
Wasit/Iraq
a.abdulkareem0903@coeng.uobaghdad.edu.iq

Ahmed Abdul Hussein Ali
Prof. Dr. in Mechanical Engineering
University of Baghdad/College of Engineering\
Mechanical Engineering
Baghdad/Iraq
ahmedrobot65@yahoo.com

ABSTRACT

Humanoids or bipedal robots are other kinds of robots that have legs. The balance of humanoids is the general problem in these types when the other in the support phase and the leg in the swing phase. In this work, the walking pattern generation is studied by MATLAB for two types of degrees of freedom, 10 and 17 degrees of freedom. Besides, the KHR-2HV simulation model is used to simulate the experimental results by Webots. Similarly, Arduino and LOBOT LSC microcontrollers are used to program the bipedal robot. After the several methods for programming the bipedal robot by Arduino microcontroller, LOBOT LSC-32 driver model is the better than PCA 96685 Driver-16 channel servo driver for programming the bipedal walking robot. The results showed that this driver confirms the faster response than the Arduino microcontroller in walking the bipedal robot. The walking pattern generation results showed that the step height for 17 degrees of freedom bipedal robot increases approximately (20%) than 10 degrees of freedom bipedal robot, which decreases the step period by about (7%). Also, the time interval of the double support phase for 17 degrees of freedom bipedal robot increases approximately (11%) with decreases step length approximately (33% on X-axis) and (16% on Z-axis).

Keywords: Experimental walking pattern, simulation walking pattern, simulation degrees of freedom robot, and experimentally degrees of freedom robot.

دراسة محاكاة وعملية لتوليد خطوات مشي لعدد من درجات الحرية لروبوت ثنائي الأرجل

أ.د. أحمد عبدالحسين علي
أستاذ دكتور
قسم الهندسة الميكانيكية/ كلية الهندسة/ جامعة بغداد

*** علي فوزي عبدالكريم**
طالب دكتوراه/مرحلة البحث
جامعة بغداد/كلية الهندسة/ قسم الهندسة الميكانيكية

الخلاصة

الروبوتات البشرية او الروبوتات ذات الارجل هي احدى انواع الروبوتات ذات اقدام. من اهم المشاكل التي تواجه هذا النوع من الروبوتات هي مشكلة الاتزان، خصوصاً عندما يكون احد الاقدام مثبت على الارض والقدم الاخرى في حالة تأرجح. في هذا العمل تم دراسة توليد خطوات المشي بإستعمال برنامج الماتلاب لنوعين من انواع الروبوتات من حيث درجة الحرية، روبوت

*Corresponding author
Peer review under the responsibility of University of Baghdad.
https://doi.org/10.31026/j.eng.2020.12.01

Article received: 8/7/2020
Article accepted: 9/8/2020
Article published:1/12/2020

ذو 10 درجة حرية و الاخر ذو 17 درجة حرية. كذلك تم استعمال نوعين من المتحكمات وهي اردوينو و LOBOT LSC-32 ببرمجة الروبوت ذو قدمين. بينت النتائج ان النوع الثاني من المتحكمات يعطي سرعة استجابة اسرع من النوع الاول. اما بالنسبة لارتفاع الخطوة فيكون في الروبوت ذو 17 درجة حرية اعلى بنسبة 20% من الروبوت ذو 10 درجة حرية مع انخفاض نسبة وقت الخطوة بنسبة 7%. اما بالنسبة لوقت الخطوة عندما تكون القدمين على الارض للروبوت ذو 17 درجة حرية فيزداد بحوالي 11% مع انخفاض طول الخطوة تقريبا 33% بإتجاه X و16% بإتجاه Z.

الكلمات الرئيسية: خطوات مشي عملي، محاكاة خطوات المشي، محاكاة درجة الحرية للروبوت ودرجة الحرية عمليا للروبوت.

1. INTRODUCTION

A bipedal robot or humanoid is another type of robot, and it has two legs. It is also a significant replacement for the active robot because it can be moved on the unpaved land. It is also the most difficult than other types of robots to stability during walking or when the first leg in the swing phase and the second leg on the ground. First, a brief history of developing the robot's design and control is studied (**Bräunl T., 2003**). **(Kemalettin E. et al., 2002**) designed a foot-mounted zero moment point ZMP sensor based on FSR (force-sensing resistors) and ZMP data obtained from bipedal robot Mari-2 and Mari-1. Also, they compared the ZMP data and gait generation between human subjects and bipedal robots.

(Shuuji K., 2003) introduced an approach of a humanoid walking pattern generation by using preview control of the ZMP. He proposed that a bipedal robot's dynamic is shaped like a running mass on a table that gives an available description to explain ZMP. So, it's also shown that a preview controller can be used to compensate for the ZMP error created by the difference between the rigid multibody model and the simple model. (**Nima Fatehi et al., 2010**) analyzed ZMP for the passivity-based humanoid. The humanoid has been simulated by using MATLAB/Simulink. Also, stable walking is studied for a specified walking method, which depends on passivity-based walking with ankles and hips actuated, and knee joints are estimated passive.

(**Shuuji Kajita et al., 2010**) developed foot force controllers on the joint position servo and a body posture controller. By applying this force/posture control, the bipedal robot system as a simple linear inverted pendulum model LIPM with ZMP delay is regarded. They studied a tracking controller design for walking stabilization and sustained it by preliminary experiment. For more reliable and realize faster walk-in outdoor, the LIPM tracking controller must be improved. **(Juan A. C. et al., 2016**) considered a new online walking control that represents the gait pattern depend on our suggested foot placement control applying the real center of mass CoM state feedback. The analytical solution of foot position is estimated depending on the LIPM to reject external disturbances and increase walking velocity.

(Tolga Olcay et al., 2017) studied the walking trajectory generation method and design of a biped robot. They used different ways for the stability of a bipedal robot, such as ZMP and LIPM. The joint angles achieved by using inverse kinematics from the generated trajectories were implemented on the robot. They concluded that the robot trunk movements were inadequate margins in both coronal and sagittal planes, and the bipedal walking robot can walk stably. A multi-level system, where the same reinforcement learning (RL) theory is studied to learn the configuration of humanoid joints (poses) that allow it to stand with balance and in the second level, they obtained the sequence of poses that allow it leads the furthest distance in the shortest time while keeping a straight path and avoiding falling as illustrated in **(Cristyan R. Gil et al., 2019**).

(Chengju Liu et al., 2020 (1)) developed a foot positioning compensator FPC for a bipedal robot to retrieve stability during continuous walking. Also, FPC is designed to improve the robustness

of humanoid, which can modify step duration online and predefined step position with sensory feedback. In addition, FPC is used to assist the bipedal robot in recovering the walking position and rejecting external disturbance. The challenge of adaptive locomotion addressed by achieving dynamic movement primitive DMP in a bipedal walking robot's workspace is discussed in (**Chengju Liu et al., 2020 (2)**). Besides, they presented an adaptive humanoid control that uses sensory feedback to regulate DMP factors. This workspace estimation allows movements to be created, such as the DMP factors, involving the height of the hip joint, stride, forward velocity, and foot clearance, directly related to the walking pattern. (**Ali F. Abdul Kareem and Ahmed A. Ali, 2020**) studied the robust stability control for three models of LIPM bipedal robot. They found that the three masses and two masses LIPM are the better performance than one mass LIPM.
The structure of this paper is divided into five sections. Section 1 presented an overview of the walking pattern generation of a bipedal robot. Section 2 describes the walking pattern generation equation and the simulation of the KHR-2HV simulation model by Webots. Section 3 details the design of a bipedal robot in the experimental work. Section 4 presents the results and discussion of the experimental pattern generation for 10 DoF and 17 DoF bipedal robots. Finally, section 5 gives the conclusions of this work.

2. THEORETICAL PART

2.1 Walking Pattern Generation Equations

In this section, the fixed zero moment point ZMP and linear inverted pendulum model are used to generate the walking pattern (**T. Olcay and A. Özkurt A., 2017**). The approach used in this work depends on determining the CoM position with zero moment point reference. This method hypothesizes that all masses concentrated in the bipedal robot's CoM and leg's mass should be much less than that of the robot trunk, as shown in **Fig. 1**. The equation of zero moment point with the center of mass positions can be written from acceleration torque balance and gravity torque as follows:

$$p_Z = c_Z - \frac{c_Y}{g}\ddot{c}_Z \tag{1}$$

$$p_X = c_X - \frac{c_Y}{g}\ddot{c}_X \tag{2}$$

A point describes zero moment point on the supporting foot $(p_Z, p_X, 0)$ in the Z and X-axis and $p_y = 0$, the position center of mass is described by (c_Z, c_X, c_Y) in the Z, X, and Y-directions, respectively, g is the gravity constant, the fixed height of the center of mass c_y = Y and m= mass of the bipedal robot.

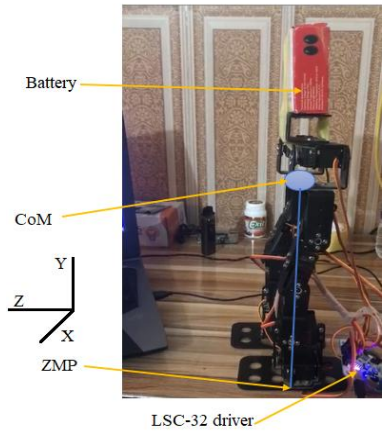

Figure 1. Linear inverted pendulum model of a bipedal robot.

For robot stability, the zero moment point should be on the supporting foot area while the swing foot is moving. When both feet are on the ground in the DSP, the zero moment point moves from one foot to another. The action is repeated in walking. Therefore, the reference of the zero moment point trajectory can be used for generating the walking pattern. This assumption says that the zero moment point is always in the middle of the supporting foot and changes quickly to the other foot during walking. (**T. Olcay, and A. Özkurt, A., 2017**) suggested that reference CoM c_Z^{ref}, c_X^{ref} are assumed as Fourier series as illustrated in Eq. (3) and Eq. (4), and the reference ZMP p_Z^{ref} and p_X^{ref} are expressed the odd functions with a period T. Therefore, the equations of the reference center of mass trajectory c_Z, c_X are:

$$c_z^{ref} = \frac{B}{T_0}\left(t - \frac{T_0}{2}\right) + \sum_{n=1}^{\infty} \frac{BT_0^2 w_n^2(1+cosn\pi)}{n\pi(T_0^2 w_n^2 + n^2\pi^2)} sin\frac{n\pi t}{T_0} \quad (3)$$

$$c_x^{ref} = \sum_{n=1}^{\infty} \frac{2AT_0^2 w_n^2(1+cosn\pi)}{n\pi(T_0^2 w_n^2 + n^2\pi^2)} sin\frac{n\pi t}{T_0} \quad (4)$$

Where c_Z^{ref}, c_X^{ref} are reference CoM in Z and X-direction respectively, T is step period, A is the distance between the center of the feet in the x-direction, B is the distance of step in the Z-direction and $w_n^2 = \frac{g}{c_y}$.

2.2 Simulation of Bipedal Robot by Webots

The walking rotation angles were set to zero to confirm the bipedal robot's stability when it is in the DSP. Afterward, the simulation results indicate experimental results. When the KHR-2HV simulation model is in the right ankle push-off phase, the sagittal plane's gait cycle is shown in **Fig. 2**. The bipedal robot is a link to a rigid body system. All motions of the links of a bipedal robot are used to confirm the balance. Hence, to stable the bipedal robot, the momentum of a part about CoM must be equal to zero. So, the above states are utilized to stability the KHR-2HV simulation model because the momentum on the right-hand side of CoM is equivalent to the momentum on the left-hand side. To confirm the bipedal robot's stability during SSP, when the right shoulder and the right leg move to the backward direction, the left shoulder and left leg must be fixed or move to the forward direction. A walking cycle can be divided into SSP and DSP, as shown in **Fig. 2**.

When the robot walks, all the angles slider begins to move, except the head slider remains zero. Therefore, the movement of the humanoid robot is similar to the human movement. From the figures, there is a relationship between the movement of the arms and the legs. This relationship is used to achieve the stability of the bipedal robot. That's mean the summation of linear momentum and angular momentum about the CoM are zero. The below figures have some terms, where: Hip represents to roll hip joint, Leg1 represents to pitch hip joint, Leg 3 represents to knee joint, ankle represents to pitch ankle joint, foot represents to roll ankle joint, arm represents to elbow joint, and Hand represents to wrist joint. The offset was adjusted, such as the resulting zero moment point for the ideal linear inverted pendulum dynamics lies within the footprint for all tested walking patterns. As the center of mass automatically follows the capture point.

Fig. 3 shows the step of the KHR-2HV simulation model in the double support phase. The center of mass and capture points are shifted from the initial center of mass position to the final center of mass position, and the desired time per footstep is used by the two control algorithms (**J. Englsberger et al., 2011**). **Table 1.** provides an overview of the angles of the KHR-2HV

simulation model's joint when the right leg in the swing phase and the left leg in the swing phase. From **Table 1** the angle of the head joint is 0° because it remains in the same direction at the movement. At the beginning of the movement, the left roll hip joint rotates approximately (5.15°, 5.7°) when the right leg in the swing phase and returned to (-12°, -12°) when the left leg in the swing phase.

Afterward, the right roll hip joint rotates (12°, 10.88°) when the right leg in the swing phase and returned to (-6.87°, -6.87°) when the left leg in the swing phase. The roll hip joint moves with small angles to confirm the stability and prevent the robot from falling in the right or left direction. When the walking in the forward direction, the right pitch hip joint begins to rotate (-33.23°, -18.33°) when the right leg in swing phase and (-31.51°,-31.51°) when the left leg in swing phase. After that, the right pitch knee joint begins to lift the below part of the right leg with (105.42°, 81.36°) when the right leg in swing phase and changed to (59.58°, 59°) when the left leg in the swing phase. Finally, the right pitch ankle joint rotates (70.47°, 63°), and the right roll ankle joint rotates (-12°, -11.45°) when the right leg in the swing phase and to complete the step.

Besides, to complete the gait cycle, the right pitch ankle joint rotates (34.95°, 34.95°), and the right roll ankle joint rotates (6.87°, 7.44°) when the left leg in the swing phase. **Fig. 2** shows the gait cycle of the KHR-2HV simulation model. When the left leg begins to lift, the right arm is moved in the forward direction until the left leg arrives at the ground. Afterward, the right arm is returned to the back when the right leg begins with rising and completed the gait cycle. The movement of the right arm is utilized to confirm the stability of the KHR-2HV simulation model. **Fig. 3** shows the step of the KHR-2HV simulation model. In this simulation, thirty-two steps are used to achieve the results.

The data were normalized and simulate by Webots software. The KHR-2HV takes approximately two seconds to complete the gait cycle and around 4 seconds to complete the gait cycle. To complete thirty-two steps, the KHR-2HV takes (64s) in the Webots program. The simulation results were performed using the KHR-2HV simulation model by Webots, which is a 3-D dynamic robotics simulator. **Table 2** compares the servomotors' deviation for the KHR-2HV simulation model between the right leg and left leg in the swing phase. The deviation of the servomotors in the right pitch hip joint, knee joint and pitch ankle joint when the right leg in the swing phase is considerably high compared with the left leg from the below table. This difference was caused by the legs' movement, where the left leg moved before the right leg to complete the step.

Fig. 4 shows the walking pattern in X-axis, Y-axis, and Z-axis with the translation movement step. Walking patterns were generated for the KHR-2HV simulation model, as shown in **Fig. 4 and Fig. 5**. KHR-2HV bipedal robot has weight and height 1,374g and 350mm, respectively. Also, it has 17 DoFs that consists of five servomotors in each leg. The KHR-2HV simulation model almost fell as it stumbled and walked unstably. This instability was caused by the dynamic center of mass motion from modifiable walking pattern generation required to perform the given footstep command (**Y. D. Hong, 2019**). The deviation of the CoM and ZMP walking pattern is shown in **Table 2.** because of the deviation that happened in the servomotors. The zero moment point in the foot center might be desirable during a step whereas a discontinuity at the transition a support phase.

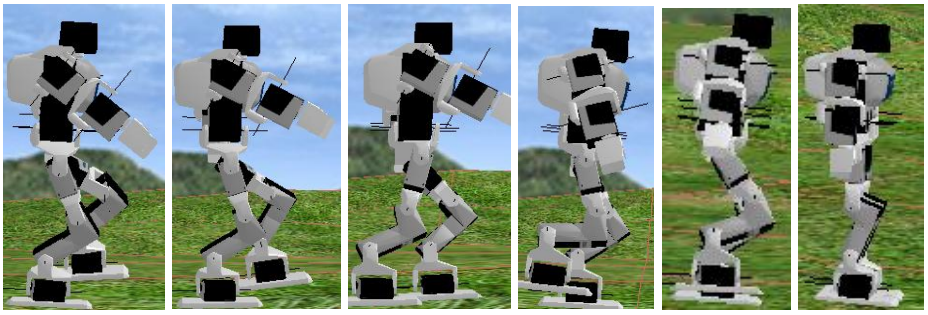

Figure 2. Gait cycle of the KHR-2HV robot in the sagittal plane by Webots program.

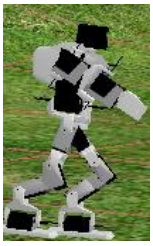

Figure 3. The step of a KHR-2HV simulation model by Webots program.

Fig. 5 provides an overview of the relationship between the X-axis, Y-axis, and Z-axis with the number of steps for the KHR-2HV simulation model in the rotation movement. The bipedal robot rotates about the fixed axis as a rigid body in X-axis, Y-axis, Z-axis, and the angle. The KHR-2HV simulation model begins to walk when the X-axis and Y-axis magnitudes are 0.882m and 0.3323m, respectively. So, the Z-axis magnitudes are approximately equivalent to the Y-axis magnitudes, as shown in **Fig. 5**. The bipedal robot is a rigid body system, where it has two motions, translation and rotation. In this simulation, the KHR-2HV simulation model walks thirty-two steps, where it begins from (0.2824m, 0.216m, and -0.516m) for (X_i,Y_i, Z_i), respectively, as shown in **Fig. 5**.

Table 1. Angles of the KHR-2HV simulation model's joints by Webots program.

No.	Movement	KHR-2HV Robot Joint Angle (°)	
		From (Right Leg in Swing Phase)	To (Left Leg in Swing Phase)
1	Head	0	0
2	Left Roll Hip Joint	5.15, 5.7	-12, -12
3	Left Pitch Hip Joint	26.35, 30	31.51, 31.51
4	Left Knee Joint	-59.58, -63	-102, -100.26
5	Left Pitch Ankle Joint	-34.95, -33.8	-54.43, -53.85
6	Left Roll Ankle Joint	-10.31, -9.74	6.87, 7.44
7	Right Roll Hip joint	12, 10.88	-6.87, -6.87

8	Right Pitch Hip joint	-33.23, -18.33	-31.51, -31.51
9	Right Knee	105.42, 81.36	59.58, 59
10	Right Pitch Ankle Joint	70.47, 63	34.95, 34.95
11	Right Roll Ankle Joint	-12, -11.45	10.31, 10.31
12	Left Shoulder	0, 0	0, 0
13	Left Arm	31.51, 31.51	16, 15.5

After the walking reaches thirty-two steps, the final values of (X_f,Y_f, Z_f) are (-0.52m, 0.215, and 0.08m) respectively. Approximately, the KHR-2HV simulation model walks in the X-axis (0.04m-0.06m) and the Y-axis 0.016m during the walking. The value of the distance in the Z-axis is approximately (0.04m-0.06m) during the walking. After thirty-two steps, the X-axis, Y-axis, and Z-axis magnitudes are 0.74m, 0.466m, and 0.742m, respectively. This instability was caused by the dynamic center of mass motion from modifiable walking pattern generation required to perform the given footstep command. The KHR-2HV simulation model is moved approximately 0.02 m in the three-axis in the rotation movement. **Fig. 6** shows the relationship between the rotation motion angle with the number of steps for the KHR-2HV simulation model. With hips trajectory and feet trajectory, inverse kinematic is used to determine the support and swing leg's joint angles.

Table 2. The deviation of the servomotor for the KHR-2HV simulation model by Webots program.

Joint	Left Leg in Swing Phase in (°)	Right Leg in Swing Phase in (°)
Head	0	0
Left Roll Hip Joint	0	0.57
Left Pitch Hip Joint	0	4.35
Left Knee Joint	1.74	-3.42
Left Pitch Ankle Joint	0.58	1.15
Left Roll Ankle Joint	0.57	0.57
Right Roll Hip Joint	0	-1.12
Right Pitch Hip Joint	0	14.9
Right Knee Joint	-0.58	-24
Right Pitch Ankle Joint	0	-7.47

Right Roll Ankle Joint	0	0.55
Left Shoulder	0	0
Left Elbow	-0.5	0

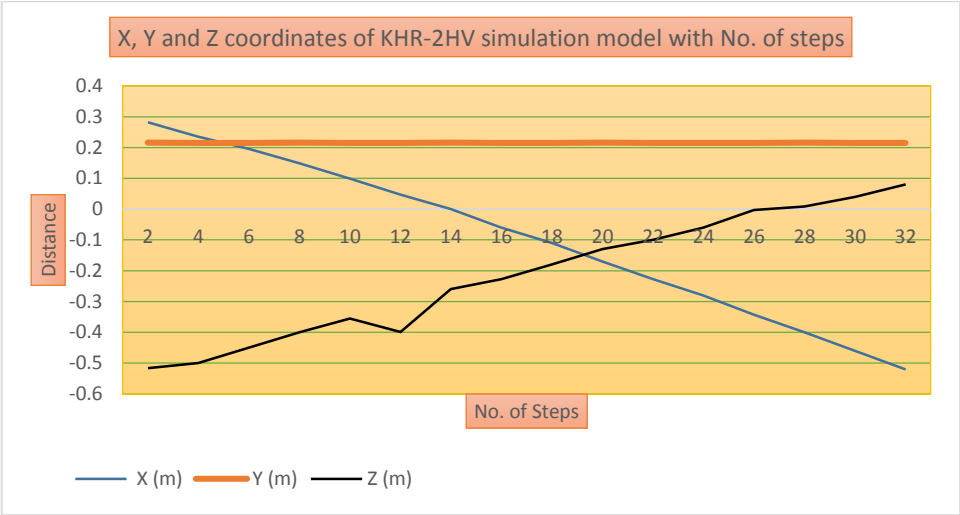

Figure 4. Translation movement of the KHR-2HV simulation model in the X, Y, and Z-axis by Webots program.

The information of the bipedal robot system is to estimate joints angles through inverse kinematic. The joints angles of the swing leg and the supporting leg's joints angles are estimated by inverse kinematics. The inverse kinematics estimates joint trajectories. Motion planning includes the motion of the feet and body. The walking of a bipedal walking robot can be estimated by controlling the foot and hip trajectories. The stability can be investigated by determining the zero moment point criteria. The X-axis points forward, the Z-axis points upward, and the Y-axis is the X-axis and Z-axis cross product. Where deviation of servo motor for KHR-2HV simulation model by Webots = lower value of angle - upper value of the angle.

Table 3. Time with the movement in the gait cycle of the KHR-2HV simulation model by Webots program.

Movement	Time (s)
Right ankle push off	0.7
Right leg in swing phase	1.5
First step	2
Left ankle push off	2.75
Left leg in swing phase	3.55
Second step	4

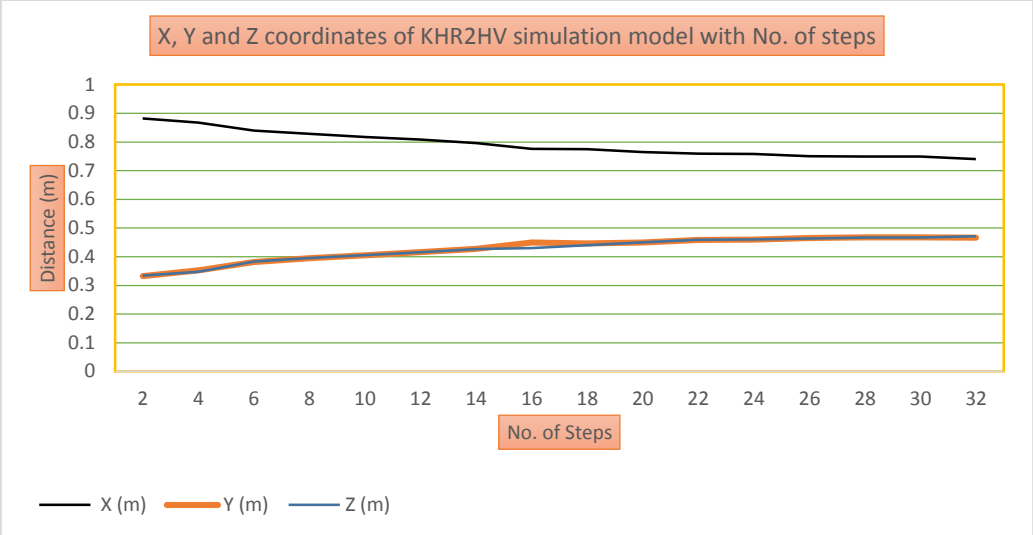

Figure 5. The rotation movement of the KHR-2HV simulation model in the X, Y, and Z-axis by Webots program.

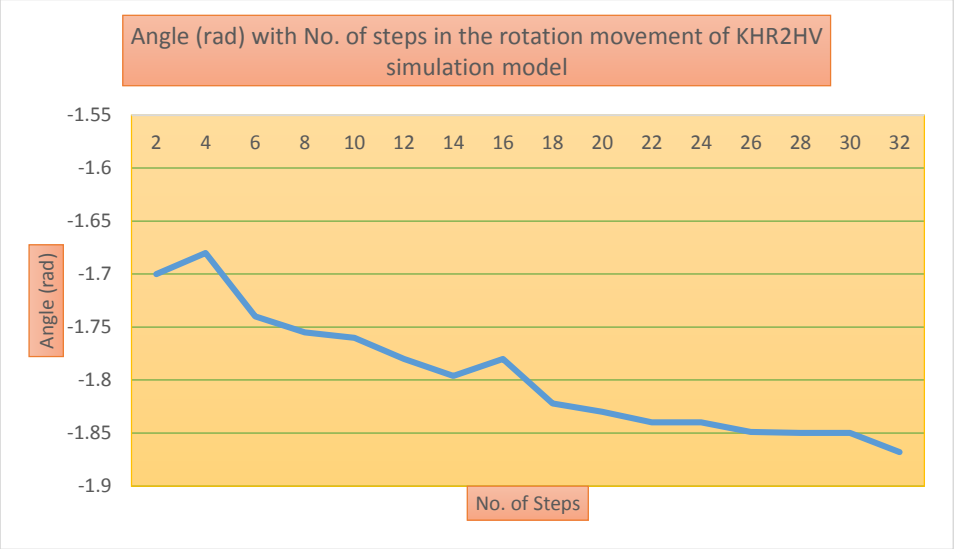

Figure 6. The rotation movement of the KHR-2HV simulation model for angle in radian by Webots program.

3. EXPERIMENTAL PART

In this section, two types of degrees of freedom DoF bipedal robot is designed. 10 DoFs and 17 DoFs bipedal robots are utilized in this work. Besides, Arduino and LSC-32 driver microcontrollers are used to programming the robots. A humanoid robot can be commonly explained as an autonomous system. This can simulate human walking motion with maintaining postural stability through the motion. A bipedal robot's design is very necessary for the bipedal robot's available performance, especially since the weight of the system imposes physical limits. The humanoid structure is highly appropriate for use in the human environment due to its advantages in being applied as human substitutes and obstacle avoidance. In this work, a bipedal robot has five DoFs for each leg, where two DoFs at the ankle joint, two DoFs at the hip joint, and one DoF at the knee joint.

The link for the humanoid robot is the main task because the servomotor is to be involved in every link (**Vaidyanathan, V. T., and Sivaramakrishnan, R., 2008**). This link will be rectangular, which contains a lower bracket and upper bracket. The servo motor will be arranged in the upper bracket and connected with the lower bracket by screws. Two brackets are connected to create a link to the humanoid robot. In this work, the bipedal robot is composed of ten Aluminum links. Each link is composed of a special structure designed to allow a low deformation and an effective torque transmission. Each link is connected to a servomotor MG996R. The links are connected, forming a humanoid of ten DoFs.

Servomotor and the lower bracket are coupled using a servomotor horn. Using the brackets, an individual joint and greater flexibility can be actuated without disturbing the other joints. To fabricate the bipedal robot, many types of bracket bipedal robots that used. The brackets are multi-functional bracket, long U bracket, short U bracket, L-type servo bracket, oblique U-type bracket, U-type robotic bracket steering gear, and foot. Metal servo arm 25T (25 toothed gear) disc metal horns are used to connect the servomotor with bracket and gives the DoF. The toothed gear is connected with the shaft of the servomotor and tighten by the screw. Steering gear brackets of robots are made of hard black Aluminum, lightweight, high hardness, sandblasting oxidation surfacing, and very high precession technology. Various holes are located on the bracket to fit most servos horns. **Fig. 7** shows the bipedal robot used in this work.

This section explains the design theory and system development of a small bipedal walking robot model with seventeen DoFs. Also, the mechanical realization and the design of small size, new, and bipedal walking robot are presented. One self-determined demand for the design is to maintain the mechanical installation as simple, lightweight, and cheap. Therefore, the humanoid is made up of several identical mechanical and electronic parts connected. Considering the cost, the hardware part was designed and depend on commercially obtainable components whenever achievable. With lightweight, inexpensive, no small motion control board commercially available at the time of conception, a microchip depends on integrating a complete control loop was designed. This section discusses the software environment and hardware design and gives a brief explanation of a self-developed motion control board's performance. Therefore, the principal factors in determining during the conceiving phase are the weight, height, and the number of joints.

The decision on the weight and height is based on keeping the humanoid manageable by a single operator. The bipedal robot is considered a two-dimensional walker. Therefore, ten DoFs are needed in the legs to permit the bipedal robot to walk the front and side road. In a fast biped walking robot, the legs' swinging creates an important moment about the vertical axis of the bipedal robot, thus resulting in a twisting motion. To counter-balance this moment, the arms have a significant weight at their disposal, where it has 2 DoFs. The controller board significantly reduces the weight and the size of the required electronics.

The microcontroller is typically computer type electrical circuitry; however, a bipedal walking robot can also be programmed by a connected computer system. It is a computer type circuitry commonly placed on one chip or PIC (Programmable Integrated Circuit), which has a memory, optional math processing, CPU (Central Processing Unit), and bus connections. Both sensors and motor are present in the robot, which are controlled by the microcontroller. The board's technical specifications are (operating voltage: 5volts, Analog input pins: 6, flash memory: 32KB, clock speed:16 MHz, size: 68.6mm*53.4mm and weight 25g). Digital (I/O) pins are characterized to connect the PWM of the servomotor with the Arduino microcontroller. Arduino UNO has 6 PWM pins (3, 5, 6, 9, 10, and 11) assigned by (~), but the Arduino MEGA has 13 PWM pins.

First, the servomotors are connected to PWM servo-driver, as shown in **Fig.** 8. The software application, such as the Arduino module working suitably for the first walking process step, but it has complicated stability in the process course. For this reason, it suggests utilizing an actuator such as D.C servomotor. It is a sixteen–channel, twelve-bit Pulse Width Modulation/servomotor driver that will drive up to sixteen servomotors over 12C with only two pins, as shown in **Fig. 8**. Two positions of control input (SCL, SDA, OE) pins and power pins (GND, VCC, V^+) on both sides are situated (**B. Earl, 2018**). Both sides of the pins are identical. Sixteen output ports are there in the PCA 96685-servo driver. Each port has three pins: GND, VCC, and the pulse width modulation pin.

To connect the PCA 96685 with a microcontroller, as shown in **Fig. 8**, the steps of the connection are (**B. Earl, 2018)**:

- 5Volts with VCC, Analog 5 with SCL, GND with GND, and Analog4 with SDA.

Be sure to attach the signal wire (commonly white or yellow) with the top row, the VCC wire (usually red) with the middle row and the ground wire (commonly brown or black) with the bottom row in the PWM 16 driver was drawing by the Fritzing program as shown in **Fig. 8**. For connecting a servomotor with PCA 96685-servo driver, most servomotors come with a standard three female pins connector (VCC, GND, and PWM) that will be connected directly to the headers on the 16-channel servo driver. The second method, the LSC-32 driver, is used for programming the bipedal robot. It is a device used to program the servomotors by Lobot Servo Control Program, as shown in **Fig. 9**. The servomotor interface of this type has over-current protection. To avoid a short circuit during the running, first, connect the servomotors to the LSC-32 servo controller and then connect the battery to the servo controller. This model was chosen because it is one of the most practical ways to describe the gait cycle for the humanoid robot. The voltage of the LOBOT LSC-32 model must be delivered between (5V to 9V). Also, this type consists of a 32-servo connection port with over current protection. Now, the humanoid robot is built by servo window action, as shown in **Fig. 9**. This servo window action is used to simulate the bipedal robot with the KHR-2HV simulation model.

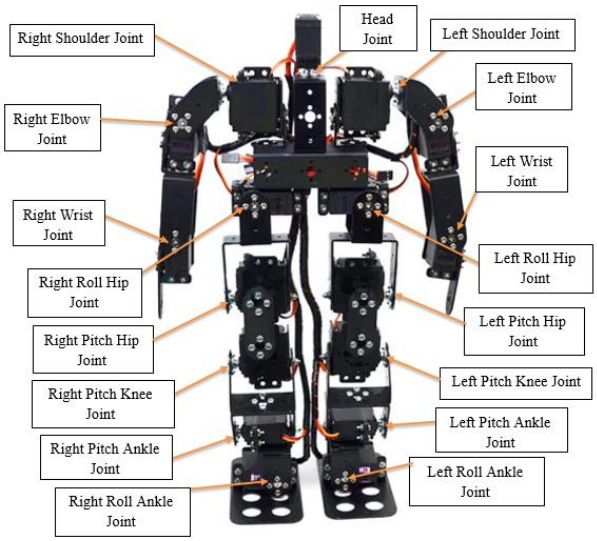

Figure 7. 17 DoF bipedal robot (**Fawzi, A. *et al.* 2020**).

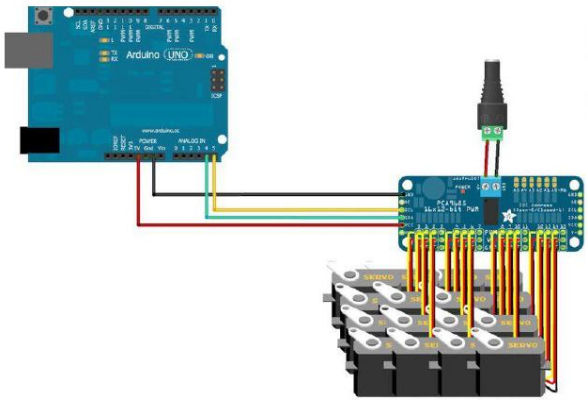

Figure 8. Connection of the 16 channel servo driver with Arduin microcontroller (**B. Earl, 2018)**.

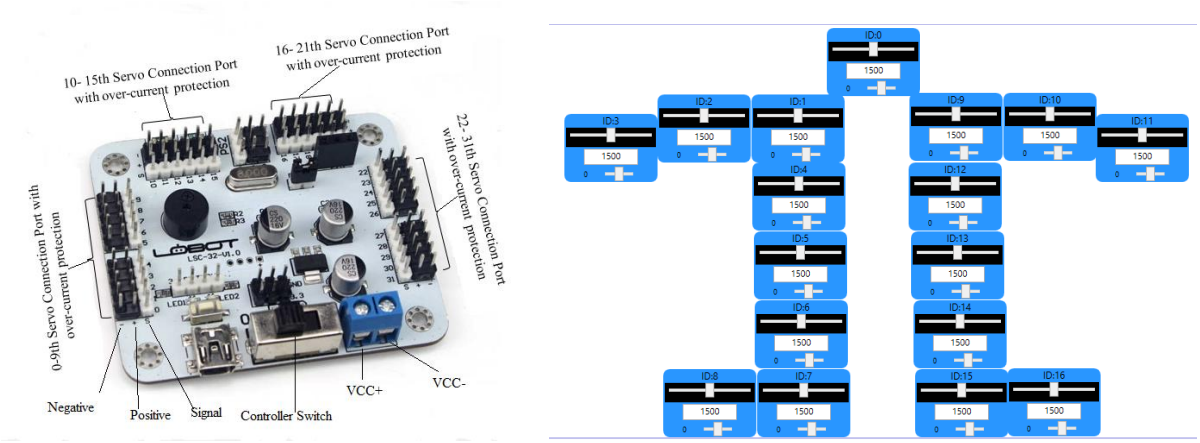

Figure 9. LSC driver and bipedal robot by Lobot Servo Control in the DSP.

4. RESULTS AND DISCUSSION

The simulation results suggest there is an association with the experimental results. Simulations were used to indicate the experimental results. After installing Lobot Servo Control software with the servo controller connected to the PC, the interface indicator turn green denotes that connecting is successful. The servomotor slider can be drag freely between 500 to 2500, where it can visually show the servomotor's rotation position at this time. Besides, there is a deviation of the servo below the slider, and it begins from (-100 to 100). To simulate the experimental results with the simulations, Eq. (5) is used. The equation of the calibration is

$$Angle\ (^{\circ}) = 0.18 \times Slider\ Value \tag{5}$$

In this section, the fixed zero moment point and linear inverted pendulum model are utilized to get the gait cycle and walking pattern. This approach depends on determining the zero moment point reference with the center of the mass position given. Also, in this approach, all masses concentrated in one point at the humanoid and the center of the mass hypothesis that the mass of legs should be much less than that of the humanoid trunk. It is also assumed that the motion of the center of mass moved in a fixed height surface. In **Fig. 12**, CoM is described as a circle (C_Z, C_X, C_Y), the fixed height C_Y is the height from CoM to the ground, and the zero moment point is represented by a point on the leg in the supporting phase ($p_Z, p_X, 0$). In zero moment point method based controlled robots, if the zero moment point is approaching the convex hull of the support area, it is concluded

the robot is going to fall, and controlling the balance stability is achieved by keeping zero moment point as far as possible for boundaries of the support area.

(**A. Goswami, 1999**) has represented foot rotation indicator FRI as an extension of ZMP, indicating the ZMP, which is equal to the foot rotation, while it lies inside the support area. Rotation of support foot happens when the foot rotation indicator exists, and ZMP reaches the support area's boundaries. Inactive robots rotation of support foot means falling, however in passivity based robots with curved soles. The support foot rotates continuously during walking. The main rule of designing a walking pattern is fulfilled to make the foot land to the ground with zero velocity w.r.t. the ground and decrease impact with guarantee stable walking of the bipedal robot and the ground. As mentioned previously, since each joint angle can be calculated from the foot's orientation and position, the generation of walking patterns in this work means to plan the foot's orientation and position. The Z trajectory is a moving footpath in the sagittal plane w.r.t. the system of base coordinates. Thus, the torso moves back and forth in turn, w.r.t. the foot.

For robot stability, when the foot in the swing phase and the other foot is supporting the ground, a zero moment point should be inside the supporting foot area. Fourier approximation zero moment point, Reference zero moment point, and Reference center of mass are estimated by MATLAB, as shown in **Fig. 10, 11, and 12,** respectively, for 10 DoFs bipedal robot. In DSP, zero moment point moves from the supporting foot to the other supporting foot in the walking. This action is called a gait cycle and repeated in walking (**S. Ito, S. Nishio, et al., 2017**). Hence, the reference zero moment point trajectory can be utilized for a generation the walking pattern shown in **Fig. 4**. This figure shows the reference ZMP trajectory in the double support phase in the X-direction.

Where the parameters used in this work, the distance between the feet is 3cm, the step period is 1.25s and $w_n^2 = \frac{g}{c_Y} = 35$. Eq. (3) and Eq. (4) describe the reference CoM trajectory for the bipedal robot. The foot segment is symmetrical and makes contact with the ground at both ends, while the ankle joint is situated at the center of this segment. The humanoid will generate the frame/ posture control of the CoM/ZMP control section and the force located by the zero moment point reference. Hence, due to mechanical compliance, it is certain that a real zero moment point behind the reference. By the preliminary experiments, the step period $T_s = 1.25s$ is determined and gives a better estimation of the zero moment point delay. When the bipedal robot stands upright, a walking pattern gives the robot's center of mass moves freely, and the posture controller keeps the upper body upright because of the control of the foot torque. In contrast, the posture controller remains the upper body upright.

One of the approximate solutions to find the ZMP trajectory with the Fourier series is suggested in the bipedal robot (**S. Ito, S. Nishio et al., 2017**). In this method, reference ZMP p_X^{ref} and p_Z^{ref} are expressed as the odd functions with a period as shown in **Fig. 10 and Fig. 11**, and reference CoM trajectories C_X^{ref} and C_Z^{ref} are hypothesized as a Fourier series for 10 DoF bipedal robots are described as Eq. (6) and Eq. (7).In DSP, the humanoid has high stability where there are many choices for designing the trajectory. Since the swing foot and support foot trajectories are designed as a cubic polynomial function (**Olcay, T. and Özkurt, A., 2017**). To keep the humanoids balanced and make the swing leg lift easily, the robots are necessary to swing in the right or left or on X-axis. The swing leg in X-direction of the robot torso is equivalent to the motion of support foot w.r.t. the robot torso (but the motion direction is opposite) occurs when the support leg is fixed on the floor during SSP.

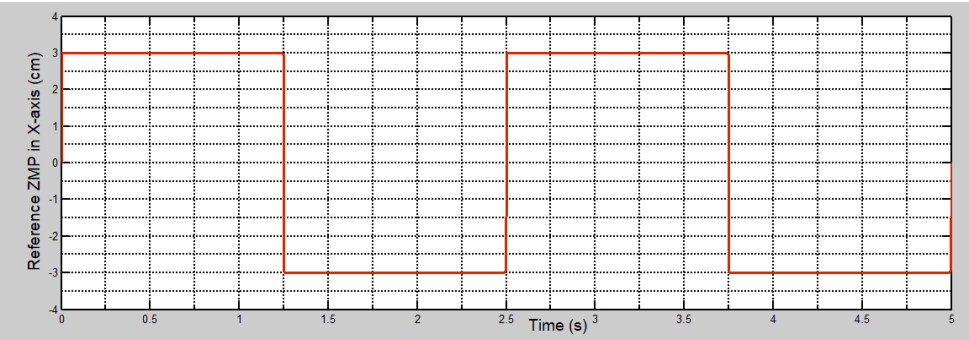

Figure 10. Reference ZMP $p_X^{ref}(t)$ in X-Direction for 10 DoFs Bipedal Robot by MATLAB.

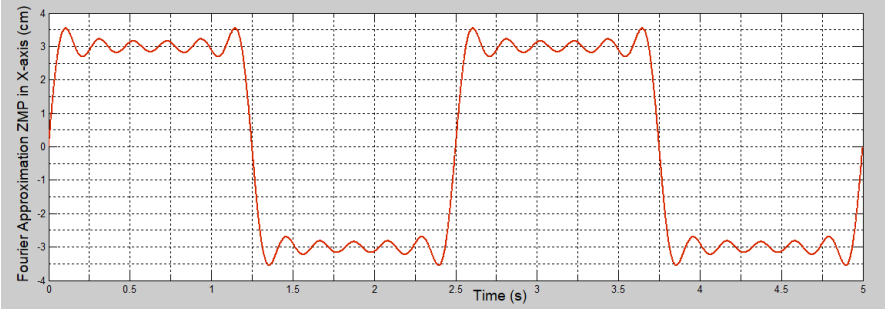

Figure 11. Fourier approximation ZMP $p_y(t)$ in X-direction for 10 DoFs bipedal robot, where n=12 by MATLAB.

$$c_X^{ref}(t) = \sum_{n=1}^{\infty}\left(\frac{328(1-cosn\pi)}{n\pi(54+n^2\pi^2)}\sin\frac{n\pi t}{1.25}\right) \quad (6)$$

$$c_Z^{ref}(t) = 4.8(t-0.625) + \sum_{n=1}^{\infty}\left(\frac{164(1+cosn\pi)}{n\pi(54+n^2\pi^2)}\sin\frac{n\pi t}{1.25}\right) \quad (7)$$

Fig. 10, 11, and 12 are plotted with step period =1.25s, the distance between the feet on X-axis=3cm, the distance between feet in Z-axis=6cm and $w_n^2 = 35/s^2$. Although these zero moment point references have the Gibbs phenomenon and a small DSP, approximate solutions of the center of mass references are appropriate for the bipedal robot. **Fig. 12** shows the reference CoM trajectory for 10 DoFs bipedal robots. Also, the gait cycle and waling generation are utilized for seventeen DoFs bipedal robots.

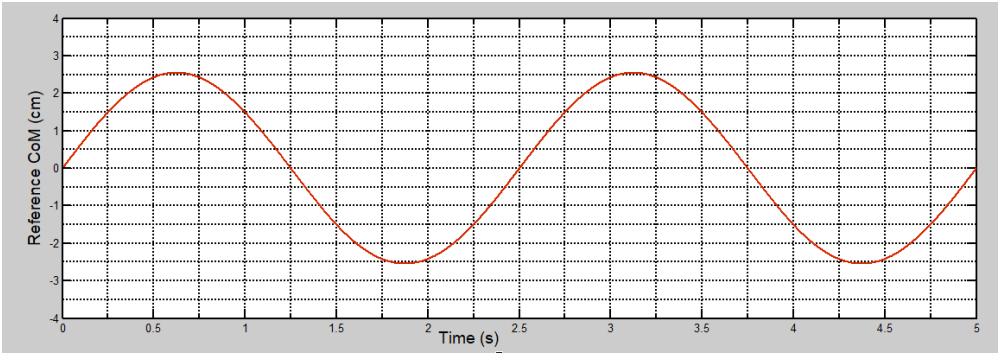

Figure 12. Reference CoM $C_X^{ref}(t)$ trajectory in X-direction for 10 DoFs bipedal robot by MATLAB.

The walking pattern control and generator are now described for 17 DoFs bipedal robots, referring to **Fig. 13**. A set of consecutive reference locations is called the walking reference trajectory for the support feet. Where the step distance between the x-direction =2.8cm, the distance between centers of the feet in the Z-direction = 5cm, T=1.35s is the step period, and $w_n^2 = \frac{g}{c_Y} = 35/s^2$.

Hence, the Fourier series is one of the approximate approaches and proposed in humanoids. Fourier approximation reference ZMP, Reference CoM trajectories, reference ZMP, and reference center of mass trajectory are shown in **Fig. 14, 15, 16** for 17 DoFs bipedal walking robot. From the inverse kinematics, the humanoid's joint angles are estimated with the swing trajectory and center of mass CoM. In this method, the odd functions with period T are assumed as Fourier series and reference zero moment point p_x^{ref} and p_Z^{ref} are expressed as reference center of mass trajectories c_Z^{ref} and c_x^{ref}. The Fourier coefficients c_Z^{ref} and c_x^{ref} for 17 DoF bipedal robot are expressed as:

$$c_x^{ref} = \sum_{n=1}^{\infty} \frac{357\,(1-\cos n\pi)}{n\pi(63+n^2\pi^2)} \sin \frac{n\pi t}{1.35} \tag{8}$$

$$c_Z^{ref} = 3.7(t-0.675) + \sum_{n=1}^{\infty} \frac{178(1+\cos n\pi)}{n\pi(63+n^2\pi^2)} \sin \frac{n\pi t}{1.35} \tag{9}$$

The linear inverted pendulum model is used to utilize the walking controller first proposed by (**S. Kajita et al., 2010, 2012**). This approach showed that the robot is not controlled in the three states, the first state when the swing leg lifts off the floor, the one foot is supported and the other in the swing phase is labeled as the second state, and the third state happens when the humanoid moved during lift-off as required by the state of the system. Besides, this approach described the complex tilting dynamics of the bipedal robot, which is estimated by the kinetics of LIPM. When the robot begins tilting in the opposite direction, the lateral velocity should not reach the threshold. The lateral velocity must be determined high adequately provide long enough the SSP (single support phase). The gait cycles are repeated in the sagittal direction. The needed lift-off states are estimated from hypothesizing the robot dynamics related to those of a LIPM and a simplified model. The kinetics and kinematic of the LIPM characterize the bipedal robot in the SSP; consequently, the base of the linear inverted pendulum is positioned in the support leg and the mass of the LIPM concentrated in the center of the humanoid as shown in **Fig. 13**.

During the DSP, the system state as lift-off must be chosen, such as the body's motion during SSP development in the required approach. The suitable lift-off state is identified to control the stability of the bipedal robot. A further hypothesis clarifies linear inverted pendulum models: during the bipedal walking robot's gait cycle, the hip's height slightly oscillates about a fixed point. The post- and pre-swing phases are commonly neglected when a bipedal robot is walking very slowly and always keeps the feet' sole parallel to the floor. Feedback control compensates for the inverted pendulum's computed motion and the errors between the real motions of the bipedal robot. There are several solutions. One solution is to apply a small correction torque and used the actuated ankle joint (**D. Wollherr, 2005**). The reference zero moment point is designed to remain within the convex hull and in the center of support foot during DSP and SSP, respectively. The generated walking pattern corresponds to the walking of four steps forward. The higher and lower frequencies are the weighting gains, and the action of this smoothing mechanism is weighing the Fourier coefficients.

The Seventeen DoFs bipedal walking robot shown in **Fig. 7** is used in this experiment. Fourier approximation ZMP, Reference center of mass, and Reference ZMP are estimated by MATLAB,

as shown in **Fig. 14, 15, 16,** respectively, for 17 DoFs bipedal robot. Also, these figures are plotted with step period =1.35s, the distance between the feet on X-axis=2.8cm, the distance between feet on Z-axis=5cm and $w_n^2 = 35/s^2$. The positional feedback needs the desired and posture location in the case of static balance control. The two segments, the body segment and a foot segment, are connected at the ankle joint positioned at the same height as the floor. The foot segment makes contact with the ground at both ends and is symmetrical, while the ankle joint is positioned at the center of this segment. However, due to the mechanical compliance, it is certain that the real zero moment point behind the reference. By the preliminary experiments, the step period $T_s = 1.35s$ that give a reasonable estimation of the zero moment point delay. The humanoid generates the force identified by the frame/ posture control of the CoM/ZMP control section and the zero moment point reference.

The posture controller remains the body above CoM upright, and the foot torque control keeps the center of mass of the robot moves freely, which is caused by a walking pattern for standing upright. For estimating the ZMP and the CoM, a frame whose origin is on the floor and Y-axis is vertical in the world frame is applied. During the SSP, when its origin on the x-axis is aligned on the leg in the support phase, the support foot's sole is set. The x-axis is set to be the average of both foot orientations, and the origin is to be the midpoint of the soles during the DSP. In the world frame's axis by the remaining track of the floor frame, the ZMP and CoM are calculated, which jumps at the moment of lift-off and touchdown. Also, the ZMP and CoM are controlled and defined w.r.t this ground frame. From one state to another, the speed of transition and/or will change in the extremities of the stability that result in the gait being dynamic or static. The common general method to the bipedal walking robot is used to keep the bipedal robot leg and arm position during walking.

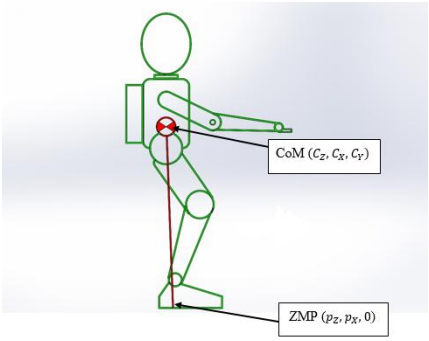

Figure 13. CoM and ZMP for 17 DoFs bipedal robots.

Kinematic obsession is the approach that used to keep the bipedal robot leg and arm position during walking because of its general utilization in bipedal robots (**T. Gabriel and M.-W. Han, 2008**). A gait cycle includes two-steps. Gaits cycle improvement for this bipedal walking robot were suggested by improving statically stable gait. Gait cycles of a bipedal robot are split into four stages and describe below. The initial states where the bipedal walking robot balanced to walk and ready are labeled as a first stage. The second stage comprises the change in CoM to its right or left depending on the support leg's position, as shown in **Fig. 14**. The gait cycle of the bipedal robot completed its first stride in the third stage. In stage four, the CoM of the bipedal robot has changed the position when the robot back to the center.

Static walking hypothesizes that the bipedal robots at any moment during the walking are statically stable. If the motion of the bipedal robot arrives at a halt at all steps, then the bipedal robot will generally be in a stable situation. Initially, the principles of the work were achieved intuitively by error and trial. A gait cycle is realized when the above cycle is repeated. The roll and hip ankle joints perform an important role while the system moves in either direction. Like other systems, instead of an ineffectual 90° turn, the bipedal walking robot can build an obtuse or an acute angle turn depending on its needs. Instead of turning and halting, the roll and pitch ankle joints' configuration enables the bipedal walking robot, which makes the system more time-efficient and bears a closer resemblance to a human walk. The below figures show smooth trajectories of reference ZMP, approximation ZMP and reference CoM with reasonable accuracy.

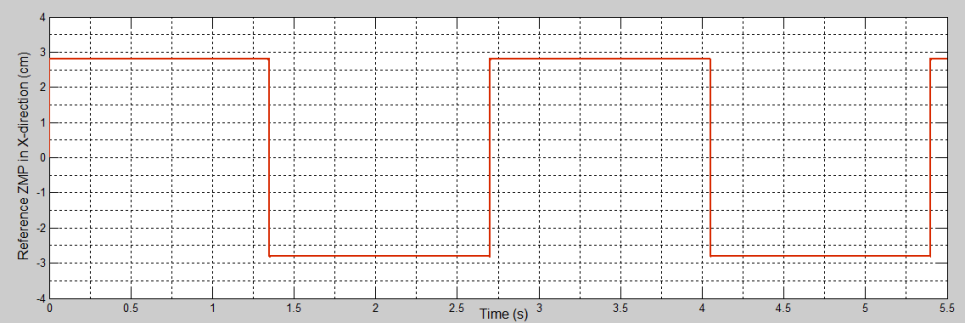

Figure 14. Reference ZMP $p_X^{ref}(t)$ in X-Direction for 17DoF Bipedal Robot by MATLAB.

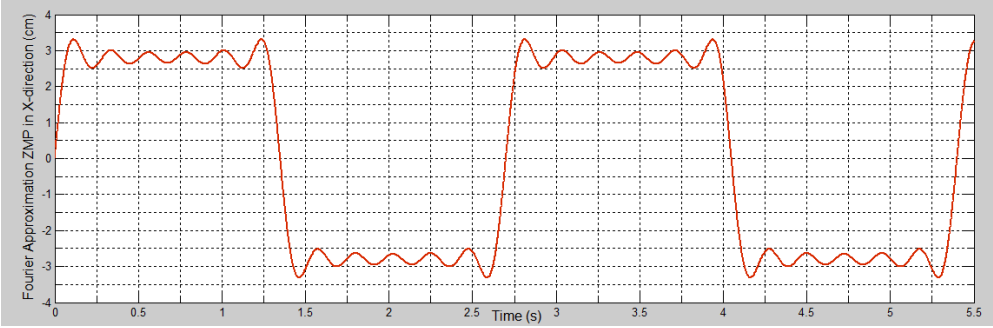

Figure 15. Fourier approximation ZMP for 17 DoF bipedal robot by MATLAB.

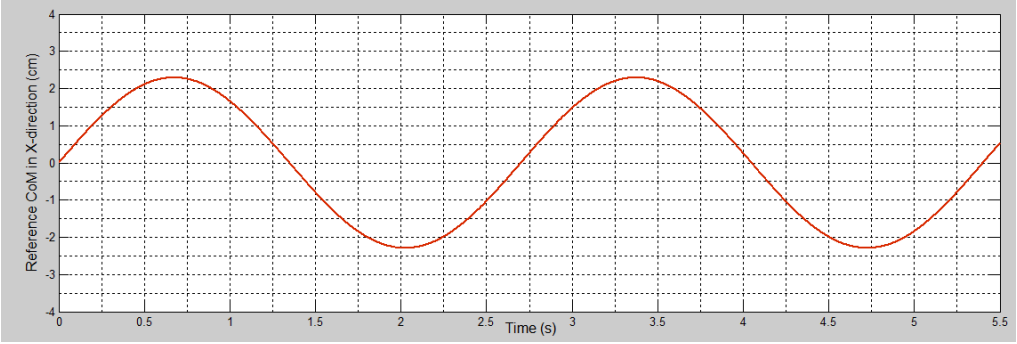

Figure 16. Reference CoM for 17DoFs bipedal robot by MATLAB.

5. CONCLUSIONS

After the several methods for programming the bipedal robot by Arduino microcontroller, LOBOT LSC-32 driver model is the better than PCA 96685 Driver-16 channel servo driver for programming the bipedal walking robot. This driver also confirms the faster response than the Arduino microcontroller in the walking of the bipedal robot. The walking pattern generation results showed that the step height for 17 DoF bipedal robot increases approximately (20%) than 10 DoF bipedal robot, which decreases the step period by approximately (7%). Also, the time interval of DSP for 17 DoF bipedal robot increases approximately about (11%) with decreases step length approximately (33% on X-axis) and (16% on Z-axis).

NOMENCLATURE

A= the distance between the center of the feet in the x-direction, m.

B= the distance of step in the Z-direction, m.

c_z, c_x, c_y= center of mass in the Z, X, and Y direction, respectively, m.

c_z^{ref}, c_x^{ref}= reference center of mass in the Z and X-direction, respectively, m.

p_z, p_x, p_y= zero moment point in the Z, X, and Y direction, respectively, m.

p_z^{ref}, p_x^{ref}= reference zero moment point in the Z and X-direction, respectively, m.

T = step period, s.

w_n^2= natural frequency, s^{-2}.

ABBREVIATIONS

CoM = center of mass.
CPU= central processing unit.
DMP= dynamic movement primitive.
DoFs = degrees of freedom.
DSP= double support phase.
FPC= foot positioning compensator.
FRI= foot rotation indicator.
LIPM = linear inverted pendulum model.
PIC= programmable integrated circuit.
PWM= pulse width modulation.
RL= reinforcement learning.
SSP= single support phase.
ZMP = zero moment point.

REFERENCES

- Goswami, 1999. Foot rotation indicator (FRI) point: a new gait planning tool to evaluate postural stability of biped robots," *Proc. - IEEE Int. Conf. Robot. Autom.*, vol. 1, no. May, pp. 47–52.
- Earl, 2018. Adafruit PCA9685 16-Channel Servo Driver Using the Adafruit Library Install Adafruit PCA9685 library Test with the Example Code : Using as GPIO Arduino Library Docs Python & Circuit Python.
- Bräunl, T., 2003. *Embedded Robotics*. Germany: Springer.
- Castano, J. A. *et al.*, 2016. Dynamic and Reactive Walking for Humanoid Robots Based on Foot Placement Control, *International Journal of Humanoid Robotics*, 13(2), pp. 1–44.
- R. Gil, Calvo, H., and Sossa, H., 2019. Learning an efficient gait cycle of a biped robot based on reinforcement learning and artificial neural networks, *Applied Sciences (Switzerland)*, 9(3).
- Chengju L. C. *et al.*, 2020. Active Balance Control of Humanoid Locomotion Based on Foot Position Compensation, *Journal of Bionic Engineering*, 17(1), pp. 134–147.
- Chengju L. *et al.*, 2020. Workspace Trajectory Generation Method for Humanoid Adaptive Walking with Dynamic Motion Primitives, *IEEE Access*. IEEE, 8, pp. 54652–54662.
- Dekker, M. H. P., 2009. Zero-Moment Point Method for Stable Biped Walking, *Report*, (July), p. 62. Available.
- Wollherr, 2005. Design and Control Aspects of Humanoid Walking Robots, *Science (80-.).*
- Erbatur, K. *et al.*, 2002. A study on the zero moment point measurement for biped walking robots, *International Workshop on Advanced Motion Control, AMC*, pp. 431–436.
- Fatehi, N., Akbarimajd, A., and Asadpour, M., 2010. ZMP analysis for dynamic walking of a passivity-based biped robot with flat feet, *ICCAS 2010 - International Conference on Control, Automation and Systems*, pp. 1419–1423.
- Fawzi, A. *et al.*, 2020. Robust Stability Control of Inverted Pendulum Model for Bipedal Walking Robot, NJES, 23(1), pp. 81–88.
- Kajita, S. *et al.*, 2003. Biped Walking Pattern Generation by using Preview, *IEEE International Conference on Robotics and Automation*, pp. 1620–1626.
- Kajita, S. *et al.*, 2010. Biped Walking Stabilization Based on Linear Inverted Pendulum Tracking.pdf, pp. 4489–4496.
- J. Englsberger, C. Ott, M. A. Roa, A. Albu-Schäffer, and G. Hirzinger, 2011. Bipedal walking control based on capture point dynamics, *IEEE Int. Conf. Intell. Robot. Syst.*, pp. 4420–4427.
- Olcay, T., and Özkurt, A., 2017. Design and walking pattern generation of a biped robot, *Turkish Journal of Electrical Engineering and Computer Sciences*, 25(2), pp. 761–769.
- S. Ito, S. Nishio, Y. Fukumoto, K. Matsushita, and M. Sasaki, 2017. Gravity Compensation and Feedback of Ground Reaction Forces for Biped Balance Control, *Appl. Bionics Biomech.*, vol. 2017.

- S. Kajita *et al.*, 2010. Biped Walking Stabilization Based on Linear Inverted Pendulum Tracking, pp. 4489–4496.
- S. Kajita, K. Miura, M. Morisawa, K. Kaneko, F. Kanehiro, and K. Yokoi, 2012. Evaluation of a stabilizer for biped walk with toe support phase, *IEEE-RAS Int. Conf. Humanoid Robot.*, pp. 586–592, 2012.
- Vaidyanathan, V. T., and Sivaramakrishnan, R., 2008. Design, Fabrication and Analysis of Bipedal Walking Robot, *Mechatronics Department of Production Technology Madras Institut of Technology India*, pp. 1–5.
- T. Gabriel and M.-W. Han, 2008. *Control of a humanoid robot based on the ZMP method*, vol. 41, no. 2. IFAC.
- Y. D. Hong, 2019. Capture point-based controller using real-time zero moment point manipulation for stable bipedal walking in human environment, *Sensors (Switzerland)*, vol. 19, no. 15.